Published in Catalysis Today, 215 (2013) 208-215
DOI: 10.1016/j.cattod.2013.03.015 *http://www.elsevier.com/*

Enhanced stability in the methanol-to-olefins process shown by SAPO-34 catalysts synthesized in biphasic medium

Teresa Álvaro-Muñoz, Carlos Márquez-Álvarez and Enrique Sastre*

Instituto de Catálisis y Petroleoquímica, ICP-CSIC.

C/ Marie Curie, 2, 28049. Madrid. Spain

Corresponding author: Dr. Enrique Sastre

E-mail: esastre@icp.csic.es

Abstract

SAPO-34 molecular sieves have been synthesized using two-liquid phase system (water/hexanol) in presence of hexadecyltrimethylammonium bromide (CTAB) or hexadecylamine (HA) as surfactant agents. This synthesis method causes higher silicon incorporation as well as greater diversification of the silicon distribution in the SAPO-34 network and decreases catalyst deactivation in the methanol-to-olefins process.

Keywords:

SAPO-34, cationic surfactant, biphasic media, methanol-to-olefins.

Published in Catalysis Today, 215 (2013) 208-215
DOI: 10.1016/j.cattod.2013.03.015 *http://www.elsevier.com/*

1. Introduction

The silicoaluminophosphate SAPO-34 (zeotype with chabazite structure) has been proven an efficient catalyst for the methanol-to-olefins (MTO) process, showing exceptionally high selectivity to lower olefins [1]. During the last few years, a large number of papers studying the influence of different synthesis parameters on the catalytic properties of this material have been published.

The influence of the structure directing agent (SDA) on the physicochemical properties and on the catalytic performance of SAPO-34 has been widely studied [2-8], demonstrating that the most efficient catalysts are obtained when tetraethylammonium hydroxide (TEOH) is used as template.

However, all these catalysts undergo rapid deactivation due to deposition of high molecular weight hydrocarbons on the pore entrances, which completely blocks the internal cages of the SAPO-34 crystals [9, 10]. Extensive studies indicate that crystallites size and morphology affect catalyst properties and applications. The catalyst performance of SAPO-34 can be strongly correlated with particle size due to the diffusion limitations of the guest molecules in the micropores [7, 9, 11-13]. In this sense, several attempts to synthesize SAPO-34 with smaller crystal size have been carried out by using different approaches: synthesis with colloidal solutions [14] or microwave synthesis [15].

In addition to the crystal size of the catalysts, distribution of silicon in the SAPO framework, which determines the acid sites concentration and strength, also influences the catalyst activity and lifetime. In some papers it has been described the positive effect of low Si content of SAPO-34 in the methanol transformation to olefins by reducing the deactivation rate and the propane production [10]. Several studies, based on theoretical calculations, have estimated the stability and structure of silica species in SAPOs [16],

postulated the mechanism of silicon substitution in SAPO materials [17] or investigated the kinetics of silicon substitution during SAPO-34 crystallization [18]. The characterization of the acidity of the different species of silicon presented in SAPO-34 has been carried out by different theoretical or experimental techniques, leading to differing conclusions. Some authors consider that the acid strength is independent of the content of Si atoms or particle size [19, 20] or that the number of strong acid sites does not change with the silicon content of the synthesis gel [21]. However, confirming the previous asseveration of Sastre et al. [22] that the acid sites in the border of silicon islands are more acidic than those next to isolated Si species, other authors, based on FTIR, neutron diffraction and NMR experiments, have described the presence of three distinct Brönsted acid sites with different strength in SAPO-34 materials [23-27].

The addition of surfactants to a two-liquid phase synthesis gel has been reported as an effective method to control the incorporation of silicon atoms to different SAPO structures like VPI-5[28], SAPO-5 [29] or SAPO-11 [30]. This synthesis procedure influences the final Si environment, promoting the modification of the mechanism of silicon incorporation into the framework and rendering samples with enhanced activity in different catalytic reactions, such as xylene isomerization or n-hexadecane hydroisomerization.

In this contribution we report the synthesis of SAPO-34 samples in a two-liquid phase medium with addition of two different surfactants, namely hexadecyltrimethylammonium bromide (CTAB) and hexadecylamine (HA), and compare their physicochemical properties and catalytic behaviour in the MTO process with those of samples obtained from conventional aqueous gel [7].

Published in Catalysis Today, 215 (2013) 208-215
DOI: 10.1016/j.cattod.2013.03.015 *http://www.elsevier.com/*

2. Experimental

2.1. Synthesis of SAPO-34 molecular sieves

Hydrothermal synthesis of SAPO-34 samples was carried out in a biphasic water-hexanol medium, using tetraethylammonium hydroxide (TEAOH, Sigma-Aldrich, 35 wt% in water) as template and with addition of a surfactant: cetyltrimethylammonium bromide (CTAB, Aldrich 95%) or hexadecylamine (HA, Aldrich 90%). Two different sources of silicon were used: colloidal silica (Ludox SM-30, 30% in water) or tetraethylorthosilicate (TEOS, Merck 98%). The gel composition was: $1Al_2O_3$: $1P_2O_5$: $0.6SiO_2$: xTEAOH: 4.4Hexanol: ySurfactant: $40H_2O$ (Table 1). For comparative purposes, a reference material was synthesized by the conventional procedure in aqueous medium according to the method published previously [7]. In all the cases, syntheses were carried out at 423 K for 5 days.

In a typical synthesis to get pure SAPO-34, the aluminium source (aluminium hydroxide, Sigma Aldrich, 100%) was added slowly to a dilute phosphoric acid solution (prepared using orthophosphoric acid, Riedel de Haën, 85%), and the mixture was vigorously stirred for 2 hours to obtain a homogeneous gel. The template (TEAOH) solution was then added drop wise to this mixture and the resulting suspension was maintained under stirring 2 hours more. After this time, a solution containing the hexanol and the surfactant was added and, immediately afterwards, the source of silicon. Finally, the mixture was stirred for about 2 hours and a uniform gel was obtained. The gel was then transferred into Teflon-lined stainless steel autoclaves with a capacity of 40 cm^3, which were heated statically at the required temperature (423 K) under autogeneous pressure for the specified period of time (5 days).

The resulting solids were collected by centrifugation, washed with water and ethanol and dried at room temperature overnight. The organic template, the water trapped within the micropores and the surfactant of the as-synthesized solids were removed by thermal treatment at 823 K under an air flow (100 ml/min) prior to catalyst testing. Complete removal of the organic molecules was assessed by thermogravimetric analysis.

2.2. Characterization

Powder X-ray diffraction (XRD) patterns of as-synthesized and calcined samples were recorded on a Philips X´PERT diffractometer using CuK_{α} radiation with a nickel filter. The textural data (pore volume and BET surface area) were determined by nitrogen adsorption measurement using a Micrometrics ASAP 2010 volumetric apparatus. Previous to measure the nitrogen adsorption/desorption isotherms samples were degassed at 623 K under vacuum for at least 20 hours. The crystal size morphology was analysed by scanning electron microscopy (SEM) using a JEOL JSM 6400 or a Philips XL30 microscopes, both operating at 20 kV.

The organic content of the samples was studied by elemental analysis with a Perkin-Elmer 2400 CHN analyser and by thermogravimetric analysis (TGA) using a Perkin-Elmer TGA7 instrument. TG analyses were carried out at a heating rate of 20 K/min under air flow. Elemental analysis for Al, P and Si was performed for calcined samples by inductively coupled plasma optical emission spectrometry (ICP-OES, Perkin-Elmer 3300DV instrument) after sample dissolution by alkaline fusion.

^{29}Si CP/MAS NMR spectra were recorded at room temperature using a Bruker AV-400-WB spectrometer operating at 79.5 MHz, with a 4 mm probe spinning at 10 kHz. A $\pi/2$

pulse of 3 μs, contact time of 6 ms and recycle delay of 5 s were used. The chemical shifts were referenced to tetramethylsilane (TMS), taken as 0 ppm.

2.3. Catalyst testing

Methanol conversion to olefins was tested at 673 K in a laboratory reactor with a continuous down flow packed bed reactor fully automated and controlled from a personal computer (PID Eng&Tech Microactivity Reference), operating at atmospheric pressure. Catalyst weight (1.0 g; 20-30 mesh pellets size) and methanol flow rate (0.150 ml/min) were varied in order to obtain a weight hourly space velocity (WHSV) of 1.2 h^{-1}. Previous to the reaction, samples were pre-treated under nitrogen flow at 723 K for 1 hour. During the reaction, nitrogen was used as an inert diluent gas and co-fed with methanol into the reactor with a constant methanol/nitrogen ratio of 1/1 mol. The reaction products were analysed on-line by gas chromatography using a Varian CP3800 gas chromatograph equipped with flame ionization (FID) and thermal conductivity (TCD) detectors, with a Petrocol DH5 0.2 capillary column and a Porapack Q 80-100 mesh packed column for separation of hydrocarbons and oxygenates, respectively.

3. Results and Discussion

The gel composition and experimental conditions used for the different samples synthesized are presented in Table 1. In all the cases, by using a biphasic media in the presence of a surfactant, it was possible to obtain materials with chabazite structure (CHA) as pure phase, except for the samples synthesized with the lowest amount of SDA (sample B-C-L) or in absence of surfactant and using TEOS as silicon source

(sample B-T). The X-ray powder diffraction patterns of the as-synthesized samples obtained with CTAB and Ludox confirm the structure type SAPO-34 (CHA structure) in all the materials (Figure 1). In all the samples, the peaks position and the intensities are identical to those reported for SAPO-34 [31], and only a slight line broadening is observed for samples prepared in the presence of surfactant compared with sample B-L, which could be related to smaller crystal size of the former samples. Samples synthesized with HA and Ludox present similar X-ray diffraction patterns (Supplementary Information). However, a clear difference is observed when TEOS is used as silicon source (Figure 2). In this case, for the same gel composition (samples prepared with y=0.144), materials synthesized with Ludox (B-C-L4 and B-H-L4), present narrower diffraction peaks than the corresponding samples synthesized with TEOS (B-C-T4 and B-H-T4), probably pointing to a smaller crystal size for the later samples. XRD patterns of calcined samples show that all the samples maintain the CHA structure after calcination, although it is remarkable that sample synthesized with CTAB and TEOS –with smaller crystal size as it will be shown below-, presents a diffraction pattern with peaks poorly defined and with relatively low intensities after calcination (Figures 1 and 2, Supplementary Information).

The chemical analyses of the different samples are presented in Table 2. It can be observed that, for the same gel composition, the amount of Silicon incorporated to the solids synthesized with Ludox increases with the surfactant concentration, for both types of surfactant (CTAB or HA). When the same amount of surfactant is used in the gel composition, samples synthesized in the presence of TEOS (B-C-T4 and B-H-T4) incorporate a significantly higher amount of silicon in the framework, compared with the corresponding samples synthesized with Ludox.

Textural properties, measured by nitrogen adsorption are presented in Table 2. It is necessary to consider that it is commonly accepted that this technique in not the most appropriate way to determine unambiguously the surface and pore volume of small pore materials like SAPO-34, and it should be used only for comparative purposes. In the case of samples synthesized with CTAB and Ludox, an initial increase in the BET surface area and the total pore volume is observed when the amount of surfactant is increased reaching maxima values for sample B-C-L4 (surfactant molar ratio in synthesis gel, y=0.144). Further increase in the concentration of surfactant in the synthesis gel produces a decrease in both values. The same variation is observed in the micropore volume. A similar trend is observed for the series of samples synthesized with Ludox and HA, although it is necessary to point out that surface area and pore volume are appreciably higher in this case. Nitrogen adsorption-desorption isotherms of the most relevant samples are presented in Figure 3 of the Supplementary Information.

The incorporation of the surfactant and the SDA to the solids has been studied by thermogravimetric and elemental (CHN) analyses (Tables 3 and 4). Thermogravimetric analyses of some selected samples are plotted in Figure 3. TGA profiles are strongly influenced by the synthesis method. In the absence of surfactant (sample B-L), three weight losses are observed. The first weight loss, at temperatures below 473 K (step I), can be attributed to desorption of adsorbed water. The second weight loss, between 673 and 823 K (step III) is due to the decomposition of the template (TEAOH) and, finally, the third weight loss at temperatures higher than 823 K (step IV) has been associated with the further removal of organic residues occluded in the channels and cages of the SAPO-34 caused by combustion. In the presence of hexanol and CTAB, the weight loss due to removal of organic compounds (T > 473 K) increases with the surfactant concentration in the gel and it is possible to observe an additional weight loss event between 423 and 673 K (step II). This additional organic content should be partially

attributed to surfactant species present in the crystals. Data of the different weight losses are presented in Table 3, where it is observed that when the amount of surfactant in the synthesis gel is increased, the total organic content also increases, mainly due to the increase of the weight loss between 423 and 673 K (region II). A simple calculation allows checking that the organic content of these samples is higher than the amount of TEA^+ cations required to fill up the void volume of SAPO-34 (which should be around 1 mol of template per chabazite cage). The organic species in excess should then be located probably on the external surface of the microcrystals.

The estimation of organic content in the samples obtained from TGA experiments can be compared with the CHN elemental analyses (Table 4). As it can be observed, values for the total amount of organic compounds in the solids determined from both techniques are in good agreement. The C/N ratio for tetraethylammonium hydroxide is 8 while that for hexadecyltrimethylammonium bromide is 19. Therefore, the C/N ratio of the samples can give an idea of the relative amounts of amine and surfactant occluded in the samples. The C/N ratio of samples crystallized in presence of hexanol and the lowest concentration of surfactant are close to 8, indicating that the organic molecules present in these samples should be mainly TEA^+ cations. For samples synthesized with higher surfactant concentration, the C/N ratio also increases suggesting that surfactant molecules are incorporated in the SAPO-34 crystals, as it was suggested by the TG analyses.

When samples synthesized with a fixed amount of CTAB (y = 0.144 mol) and different silicon source in the synthesis gel are compared (samples B-C-L4 and B-C-T4, Table 3), it can be observed that the sample prepared with TEOS incorporates a higher amount of organic compounds. The main difference in the TG profiles of both samples is observed in region II, which could indicate that the later sample incorporates a higher amount of

surfactant, as it is also confirmed by the higher C/N ratio observed for this sample (Table 4). When hexadecylamine is used as surfactant (samples B-H-L4 and B-H-T4) only minor differences are observed between both samples that present characteristics similar to those of sample B-C-L4, although with a slightly lower C/N ratio.

The morphology of the different samples has been determined by SEM (Figure 4). The properties of SAPO-34 crystals obtained with CTAB were influenced by the amount of surfactant employed. When low amount of surfactant was used (up to y = 0.144 mol CTAB), rhombohedral crystals of approximately 300 nm in size were obtained. However, the crystallite size increased for higher surfactant concentrations, reaching 1 μm for the maximum amount of surfactant used (y = 0.3, sample B-C-L7).

The nature of the surfactant also influences the crystal size of the samples. For the same concentration of surfactant, slightly larger crystals are obtained when the neutral surfactant (HA) is used instead of CTAB (Figure 5, samples B-H-L4 and B-C-L4). In addition, a notable effect is also observed when the source of silicon is changed. The use of TEOS leads to smaller crystal sizes than Ludox when the same gel concentration is used (Figure 5, samples B-H-T4 and B-C-T4).

Although it is not easy to determine, in all cases the SEM photographs show that samples are quite uniform, which may suggest that the presence of amorphous material, if any, should be limited.

These results evidence that not only the surfactant concentration, but also the silicon source, play an important role in the crystallization process, for the positively charged ions can modify the morphology of crystals. This suggests a specific interaction between the positive head of the surfactant cation and the anions existing in the synthesis media.

In addition, the surfactant could also compensate partially the negative charge induced by the replacement of P by Si in the aluminophosphate framework when the SAPO material crystallizes, thus influencing silicon incorporation. In this sense, as it was mentioned previously, the amount of silicon incorporated in the SAPO-34 samples increased with the amount of surfactant in the synthesis gel. The Si/(Si+Al+P) ratio was 0.1 for the sample synthesized in the absence of surfactant and increased linearly from 0.16 to 0.25 when the CTAB molar ratio (y) increased from 0.07 to 0.3 (Table 2). Furthermore, ^{29}Si CP/MAS NMR spectra (Fig. 6) showed that the presence of the cationic surfactant caused a change on the silicon distribution in the SAPO framework. For the sample prepared without surfactant (B-L), the spectrum shows a predominant peak centred at -85 ppm, which indicates that essentially for all Si atoms the four neighbouring atoms in the second coordination shell are Al (Si(4Al) species). This shows that Si is incorporated in the alternate Al-P network by substitution of single P atoms (SM2 mechanism). Therefore, the calcined sample would contain mild acid sites in an amount equal to that of silicon. In contrast, the spectra of samples obtained with surfactant added to the gel (samples B-C-L2, B-C-L4 and B-C-L7), consist of a broad envelope in the -80 to -120 ppm range, corresponding to several resonances due to different Si(nAl) environments (n=0-4), in which the Si atoms are surrounded by n Al and 4-n Si atoms. Therefore, in these samples Si incorporation occurs not only by SM2 mechanism but also by simultaneous substitution of a pair of adjacent Al-P atoms (SM3 mechanism). The maxima of these envelopes are in the -90 to -100 ppm range, which indicates that most of the Si atoms are surrounded by 2 to 4 Al atoms (2 to 0 Si atoms, respectively). Therefore, these samples possess both isolated Si atoms and very small silica domains, but no large silicon islands. Hence, the concentration of acid sites would be slightly lower than that of silicon. On the other hand, the average acid strength would

be higher than that of the sample synthesized in the absence of surfactant, for the acid strength of bridging hydroxyls (Si-OH-Al) is known to increase as the number of Al atoms in the second coordination shell of Si decreases.

Samples synthesized with the same gel composition as sample B-C-L4, but with different surfactant or silicon source (B-H-L4, B-C-T4 and B-H-T4), present different NMR spectra (Figure 7). Sample synthesized with hexadecylamine (B-H-L4) shows a Si distribution quite similar to the one obtained for sample B-L, synthesized without surfactant, probably because the amount of Si incorporated in the solid is the same, lower than for sample B-C-L4 (Table 2). In this case, only a peak centred at -89 ppm is observed, indicating the presence of Si(4Al) species almost exclusively. In contrast, when TEOS is used in the synthesis gel as Si source, in the presence of CTAB, as it was mentioned previously the amount of Si incorporated to the solid is higher and the NMR spectrum shows the characteristic broad peak attributed to different Si(nAl) environments (n=0-4), in which the Si atoms are surrounded by n Al and 4-n Si atoms, similar to the one observed for sample B-C-L7, with a similar Si content in the solid. It is important to consider that both the presence of defects in the crystals, and the presence of amorphous material in the solids could contribute to broaden the NMR spectra. In the case of samples synthesized with TEOS, the presence of crystalline defects in the calcined samples cannot be ruled out completely, as discussed above, although, from the results of SEM, the presence of amorphous material can be almost definitely discarded.

In conclusion, it is possible to control the concentration and the distribution of the Si environments by changing the synthesis parameters, especially the nature and concentration of the surfactant and the Si source.

Published in Catalysis Today, 215 (2013) 208-215
DOI: 10.1016/j.cattod.2013.03.015 *http://www.elsevier.com/*

The catalytic activity and selectivity of samples synthesized in biphasic media with Ludox and CTAB have been compared with a reference sample synthesized by using a conventional aqueous hydrothermal method [7] (Figures 8 and 9). All the catalysts showed high initial activity in the MTO reaction at 673 K (Figure 8), and under the experimental conditions used (WHSV of 1.2 h^{-1}), full conversion of oxygenates (both methanol and intermediate dimethyl ether) was obtained. Selectivity to short chain olefins ($C_2^=$-$C_4^=$) reached a nearly constant level close to 90% after ca. two hours on stream, except for sample B-C-L7, which showed a fast selectivity decay after one hour on stream (Figure 9). After several hours on stream, a fast activity decay occurred due to formation of carbonaceous deposits although selectivity to short chain olefins remained above 85%. Important differences are observed in catalyst lifetime depending on the relative amount of surfactant used in the synthesis. The sample obtained without addition of surfactant (B-L) maintained conversion level above 80% during 4 hours. This time increased with surfactant content up to y = 0.14-0.20 mol CTAB (samples B-C-L4 and B-C-l5), reaching 8 h and improving appreciably the lifetime of the reference catalyst (synthesized in aqueous medium and having a Si/(Si+Al+P) ratio of 0.17). This increase can be attributed to the increase of acid sites concentration due to higher silicon incorporation, as it was shown previously. For samples obtained with higher amount of surfactant (y > 0.2, samples B-C-L6 and B-C-L7), the catalyst lifetime decreased as the amount of surfactant increased, which might be related to two different factors. First, the increase in the Si content of the solid, which increases the number of Si(nAl) environments, being n equal to 2 or 1. These Si species are associated to acid centres with higher acid strength [22] and, therefore, are responsible of the transformation of short chain olefins to higher molecular weight compounds, which causes the catalyst deactivation. The second factor affecting the stability of the catalyst is the marked

increase of crystal size of these samples, which has been also correlated with a lower resistance of the catalysts to deactivation [7, 9, 13]. These effects are especially notable for sample B-C-L7, with the highest Si content and largest crystal size.

Catalytic results obtained with samples with the same molar amount of Si in the synthesis gel, but changing the nature of the Si source or the type of surfactant, are presented in Figure 10. Sample B-H-L4 synthesized with Ludox and HA, presents a lower life time than sample B-C-L4, synthesized with CTAB and one of the two most stable samples obtained previously. This can be related not only to the lower amount of Si incorporated in the solid (Table 2), which is preferentially located as Si(4Al) environments (Figure 7), but also to the larger crystal size of this sample (Figure 5) compared with sample B-C-L4.

It is interesting to notice that samples synthesized with TEOS as Si source (B-C-T4 and B-H-T4), are more prone to deactivation than their Ludox counterparts, showing a rapid decrease of catalytic conversion after 3 hours of reaction. In this case, the higher deactivation rate cannot be attributed to the crystal size of the catalysts because, as it was shown previously (Figure 5), these samples are synthesized with a smaller crystal size. The amount of Si in the solid is slightly higher for sample B-C-T4 than that of sample B-C-L4, but the Si environments are clearly different (Figures 6 and 7). Sample synthesized with TEOS (B-C-T4) presents a higher population of Si(2Al) and Si(1Al) centres, while sample synthesized with Ludox (B-C-L4), shows a higher number of Si(4Al) and Si(3Al) environments. As it has been mentioned previously, up to now [32] it has been commonly accepted that the strength of the acid centres associated to the Si atoms increases when the number of Al in the first coordination sphere decreases (from n=4 to n=1), so it could be possible to attribute the higher deactivation of sample B-C-

T4 to the higher acid strength of the acid centres present in this catalysts compared to sample B-C-L4.

From these data it is clear that an optimum balance between acidity (number and strength) and crystal size of the SAPO-34 catalysts is necessary to obtain more stable materials with longer life time. The synthesis of SAPO-34 by using a biphasic media and the addition of a surfactant has demonstrated to be an efficient method to control the amount and environment of the silicon incorporated into the crystalline framework and, thus, to control the catalytic performance of the solid obtained. In this sense, samples synthesized from gels containing surfactant mole ratios in the range y = 0.14-0.2 rendered the best catalytic performance based on its small crystal size and mild acidity associated to the presence of small silicon domains.

Conclusions

Different samples of SAPO-34 have been obtained by adding a surfactant to a two-liquid phase synthesis gel. Samples prepared with this methodology show a different Si distribution than that synthesized in absence of surfactant. The results showed that the use of the two-liquid phase synthesis causes greater incorporation and diversification of the silicon distribution in the SAPO-34 network and therefore, a substantial increase in the material acidity. Samples synthesized with hexadecyltrimethylammonium bromide molar ratio in the range 0.14-0.2 rendered the best catalytic performance based on its small crystal size and mild acidity.

Published in Catalysis Today, 215 (2013) 208-215
DOI: 10.1016/j.cattod.2013.03.015 *http://www.elsevier.com/*

Acknowledgements

We are thankful for the financial support of the Spanish Ministry of Science and Innovation, projects MAT2009-13569 and MAT2012-31127. TAM acknowledges CSIC for a PhD grant.

Published in Catalysis Today, 215 (2013) 208-215
DOI: 10.1016/j.cattod.2013.03.015 *http://www.elsevier.com/*

Table 1. Gel composition and synthesis conditions for the different SAPO-34 materials. Crystallization was maintained at 423 K for 5 days.

$1Al_2O_3$: $1P_2O_5$: $0.6SiO_2$: x TEAOH: 4.4Hexanol: y Surfactant: $40H_2O$

Sample	Surfactant	x	y	Si source[b]	Phase
S-TEAOH-5[a]	-	1	0	L	CHA
B-C-L	CTAB	1	0.144	L	CHA + AFI
B-C-L1	CTAB	2	0.0072	L	CHA
B-C-L2	CTAB	2	0.072	L	CHA
B-C-L3	CTAB	2	0.100	L	CHA
B-C-L4	CTAB	2	0.144	L	CHA
B-C-L5	CTAB	2	0.200	L	CHA
B-C-L6	CTAB	2	0.250	L	CHA
B-C-L7	CTAB	2	0.300	L	CHA
B-H-L4	HA	2	0.144	L	CHA
B-H-L5	HA	2	0.200	L	CHA
B-H-L6	HA	2	0.250	L	CHA
B-C-T4	CTAB	2	0.144	T	CHA
B-H-T4	HA	2	0.144	T	CHA
B-L	-	2	0	L	CHA
B-T	-	2	0	T	CHA + AFI

[a] Reference sample synthesized in aqueous medium [7]

[b] L: Ludox; T: TEOS

Published in Catalysis Today, 215 (2013) 208-215
DOI: 10.1016/j.cattod.2013.03.015 *http://www.elsevier.com/*

Table 2. Chemical composition and textural properties of SAPO-34 samples

Sample	$Si/(Si+Al+P)_{solid}$ [b]	S_{BET} (m^2/g)	V_{TOT} (cm^3/g)	V_{micro} (cm^3/g)	V_{exter} (cm^3/g)
S-TEAOH-5[a]	0.20	652	0.55	0.26	0.29
B-L	0.10	227	0.24	0.08	0.16
B-C-L1	0.15	230	0.25	0.08	0.17
B-C-L2	0.16	509	0.32	0.19	0.13
B-C-L3	0.17	523	0.34	0.20	0.14
B-C-L4	0.20	547	0.36	0.21	0.15
B-C-L5	0.21	389	0.32	0.13	0.19
B-C-L6	0.22	359	0.28	0.13	0.15
B-C-L7	0.25	246	0.21	0.07	0.14
B-H-L4	0.10	696	0.48	0.27	0.21
B-H-L5	0.11	569	0.34	0.22	0.12
B-H-L6	0.13	563	0.35	0.20	0.15
B-C-T4	0.23	152	0.18	0.05	0.13
B-H-T4	0.18	676	0.76	0.26	0.50

[a] Reference sample synthesized in aqueous medium [7]

[b] $Si/(Al+P)_{gel}= 0.15$

Published in Catalysis Today, 215 (2013) 208-215
DOI: 10.1016/j.cattod.2013.03.015 *http://www.elsevier.com/*

Table 3. Thermogravimetric analysis of the samples

Sample	Weight loss (%)				
	I	II	III	IV	Total
	T<473K	473K<T<673K	673K<T<823K	T>823K	organic
S-TEAOH-5[a]	3.1		14.2	1.8	16.0
B-L	4.6		14.8	1.3	16.1
B-C-L1	4.4	1.6	12.7	1.4	15.8
B-C-L2	5.1	6.0	10.4	1.9	18.3
B-C-L3	5.2	6.7	10.9	1.6	19.2
B-C-L4	4.9	8.4	10.5	3.2	22.1
B-C-L5	6.0	8.6	10.8	1.9	21.2
B-C-L6	2.8	11.3	10.3	2.7	24.3
B-C-L7	12.0	14.8	8.4	3.2	26.4
B-H-L4	4.2	5.9	12.1	1.9	19.9
B-C-T4	7.8	15.3	8.6	6.7	30.7
B-H-T4	5.7	5.9	11.8	3.8	21.4

[a] Reference sample synthesized in aqueous medium [7]

Published in Catalysis Today, 215 (2013) 208-215
DOI: 10.1016/j.cattod.2013.03.015 *http://www.elsevier.com/*

Table 4. Organic content of the samples

Sample	Weight %			C/N	Total organic (wt %)
	C	H	N		
S-TEAOH-5[a]	9.8	2.6	1.6	7.4	13.9
B-L	9.4	2.8	1.3	8.6	13.4
B-C-L1	10.5	2.8	1.4	8.6	14.7
B-C-L2	14.7	3.6	1.6	11.0	19.8
B-C-L3	14.9	3.5	1.6	10.9	20.0
B-C-L4	15.2	3.6	1.7	10.5	20.5
B-C-L5	15.4	4.0	1.5	12.0	20.9
B-C-L6	18.1	4.7	1.5	14.2	24.3
B-C-L7	21.9	4.9	1.4	18.4	28.1
B-C-T4	21.4	4.9	1.9	13.2	28.2
B-H-T4	13.2	3.5	1.9	8.3	18.6

[a] Reference sample synthesized in aqueous medium [7]

Figure Captions:

Figure 1. X-ray diffraction patterns of samples synthesized in biphasic media with Ludox and increasing amounts of CTAB.

Figure 2. X-ray diffraction patterns of samples synthesized with the same gel composition in biphasic media using different SDA and silicon source.

Figure 3. Thermogravimetric analyses of some selected samples synthesized with different CTAB concentration in biphasic media

Figure 4. Scanning Electron Micrographs of samples synthesized with different CTAB concentration in biphasic media

Figure 5. Scanning Electron Micrographs of samples synthesized in biphasic media with different surfactant and Si source and a constant concentration of Si in the gel

Figure 6. ^{29}Si CP/MAS NMR spectra of calcined catalysts synthesized in biphasic media with different content of Si and CTAB.

Figure 7. ^{29}Si CP/MAS NMR spectra of calcined samples B-C-T4, B-H-L4 and B-H-T4.

Figure 8. Conversion of oxygenates (MeOH and DME) vs. reaction time of samples synthesized in biphasic media with different content of Si and CTAB and a reference sample synthesized by using a conventional aqueous hydrothermal method [7]. Test conditions: T= 673 K, WHSV = 1.2 h^{-1}, 1 g of catalyst.

Figure 9. Selectivity to $C_2^=$-$C_4^=$ olefins vs. reaction time of samples synthesized in biphasic media with different content of Si and CTAB and a reference sample synthesized by using a conventional aqueous hydrothermal method [7]. Test conditions: T= 673 K, WHSV = 1.2 h^{-1}, 1 g of catalyst. Same symbols as in Figure 8.

Figure 10. Conversion of oxygenates (MeOH and DME) vs. reaction time of samples synthesized in biphasic media with different surfactant and Si source. Test conditions: T= 673 K, WHSV = 1.2 h^{-1}, 1 g of catalyst.

Published in Catalysis Today, 215 (2013) 208-215
DOI: 10.1016/j.cattod.2013.03.015 *http://www.elsevier.com/*

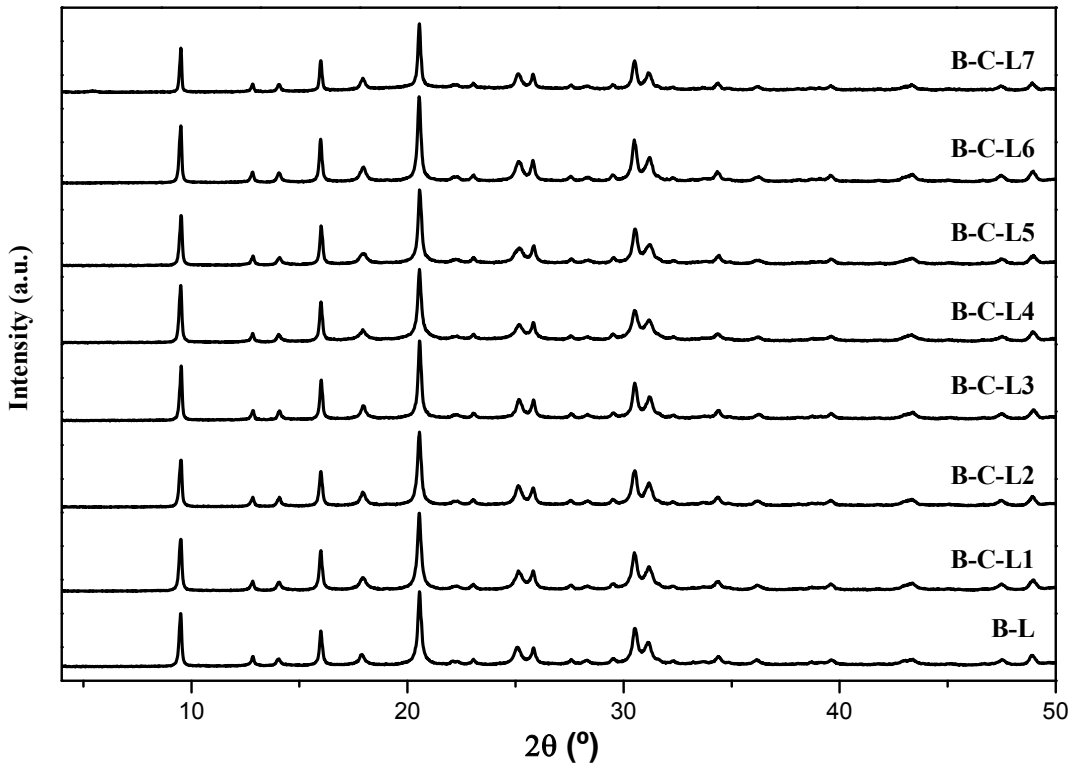

FIGURE 1

Published in Catalysis Today, 215 (2013) 208-215
DOI: 10.1016/j.cattod.2013.03.015 *http://www.elsevier.com/*

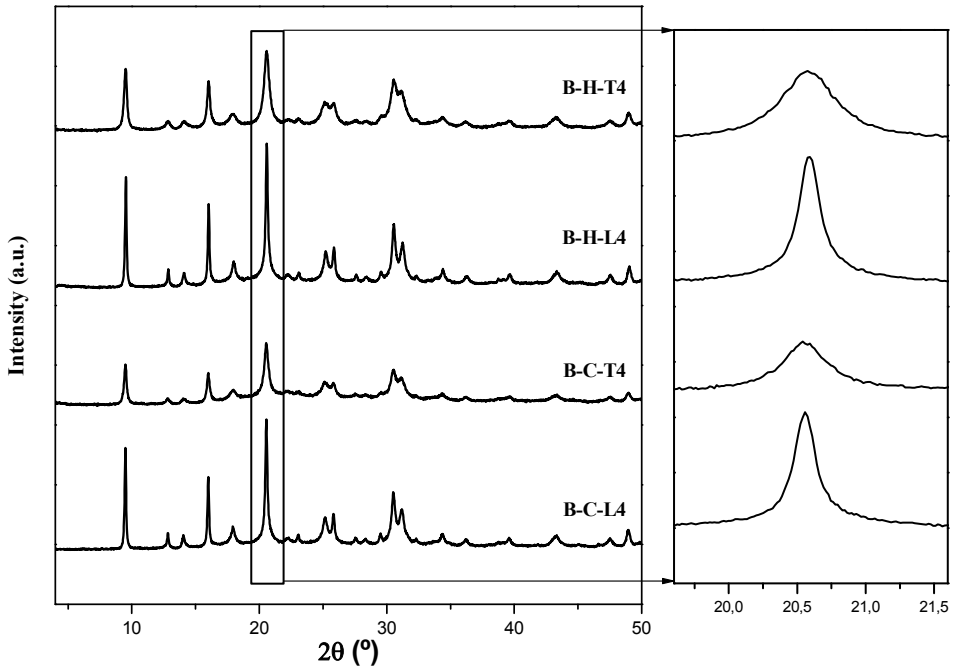

FIGURE 2

Published in Catalysis Today, 215 (2013) 208-215
DOI: 10.1016/j.cattod.2013.03.015 *http://www.elsevier.com/*

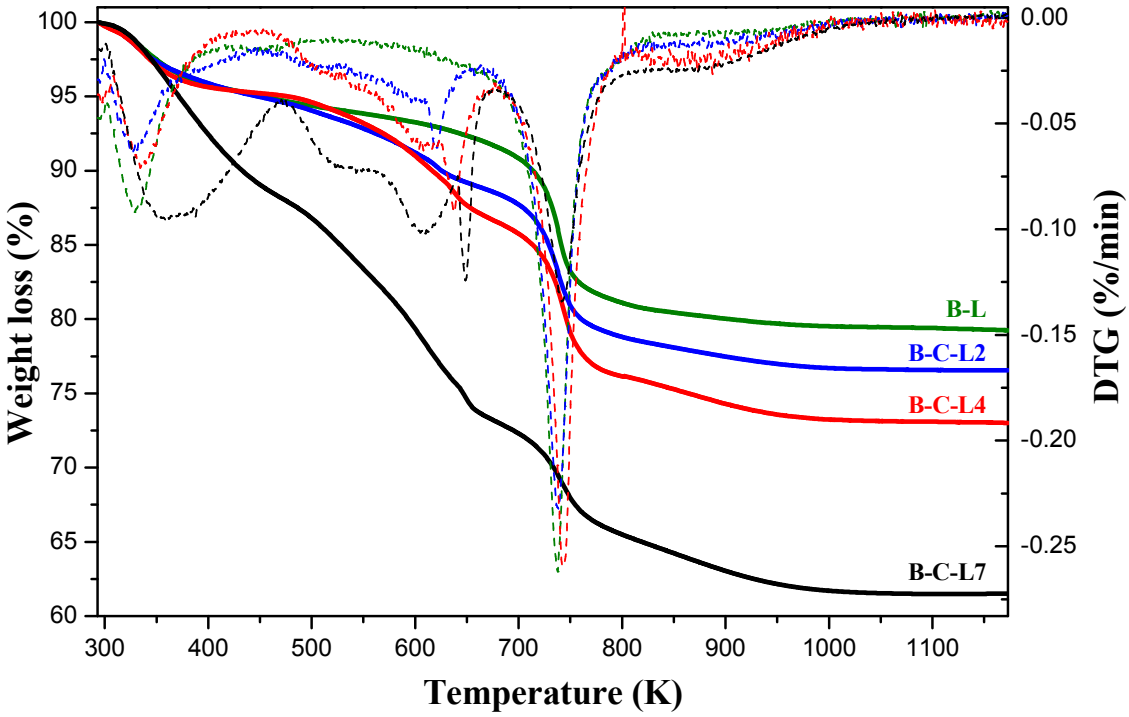

FIGURE 3

Published in Catalysis Today, 215 (2013) 208-215
DOI: 10.1016/j.cattod.2013.03.015 *http://www.elsevier.com/*

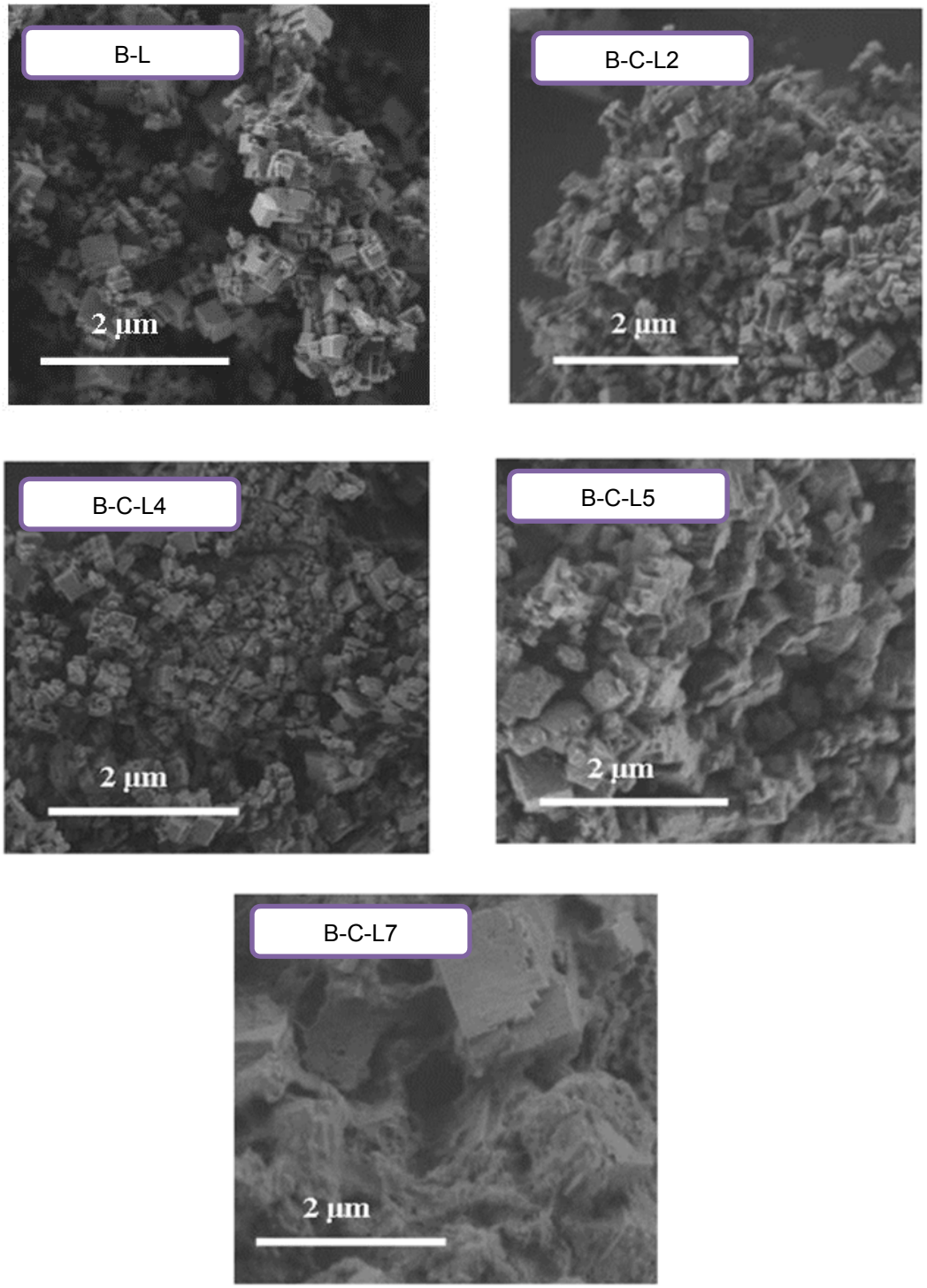

FIGURE 4

Published in Catalysis Today, 215 (2013) 208-215
DOI: 10.1016/j.cattod.2013.03.015 *http://www.elsevier.com/*

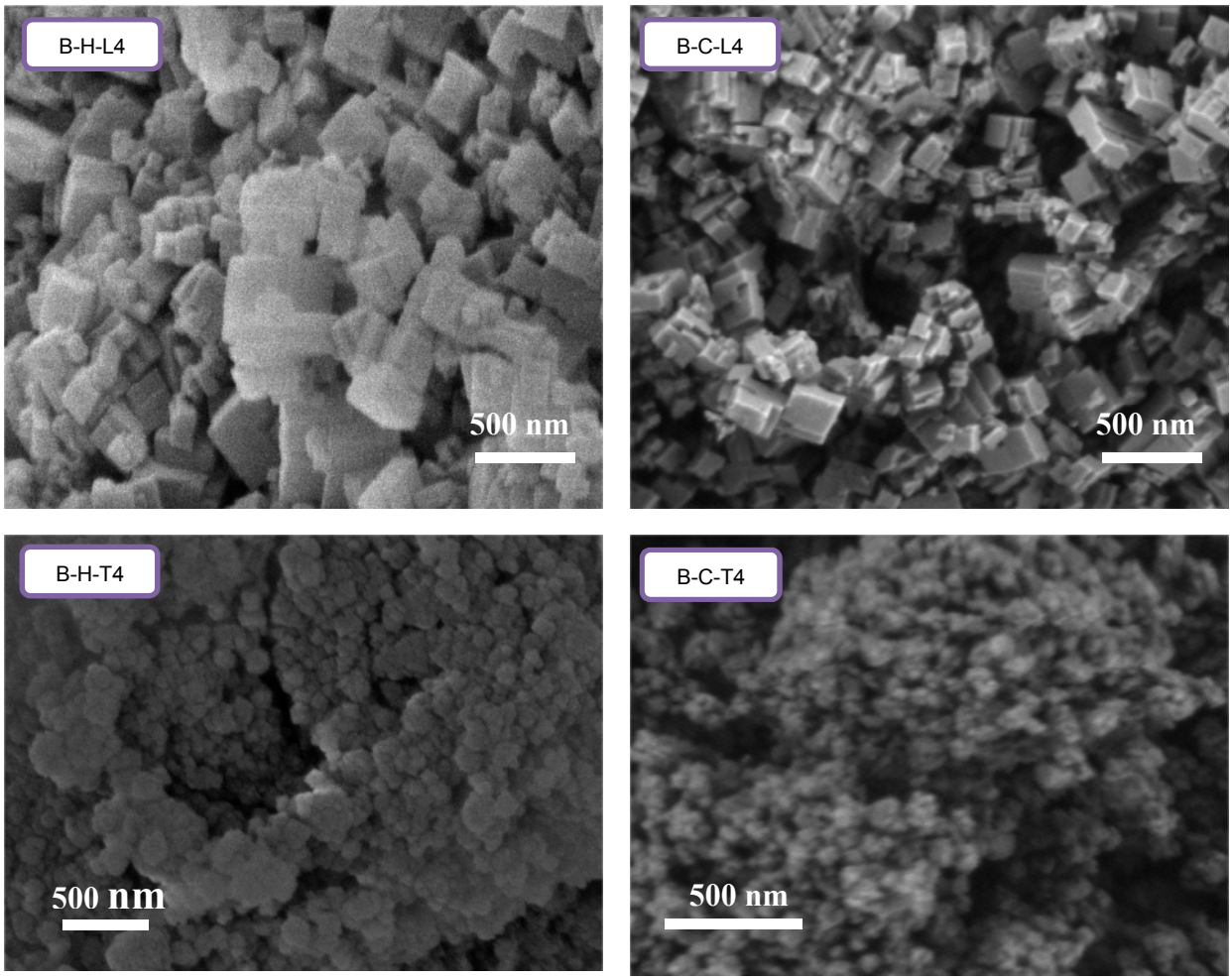

FIGURE 5

Published in Catalysis Today, 215 (2013) 208-215
DOI: 10.1016/j.cattod.2013.03.015 *http://www.elsevier.com/*

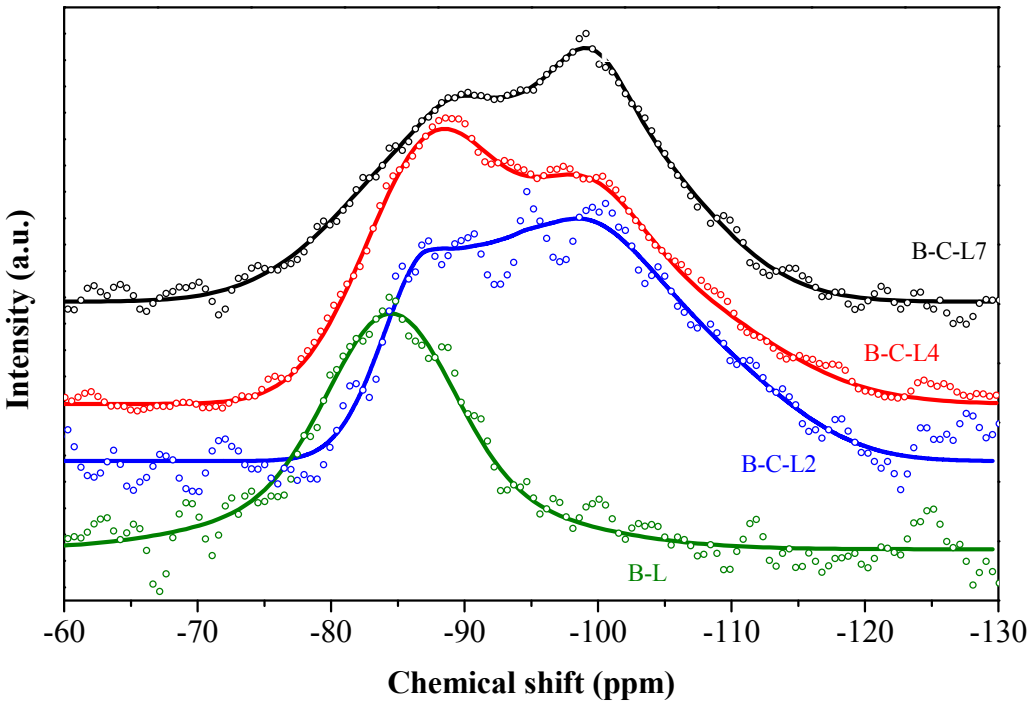

FIGURE 6

Published in Catalysis Today, 215 (2013) 208-215
DOI: 10.1016/j.cattod.2013.03.015 *http://www.elsevier.com/*

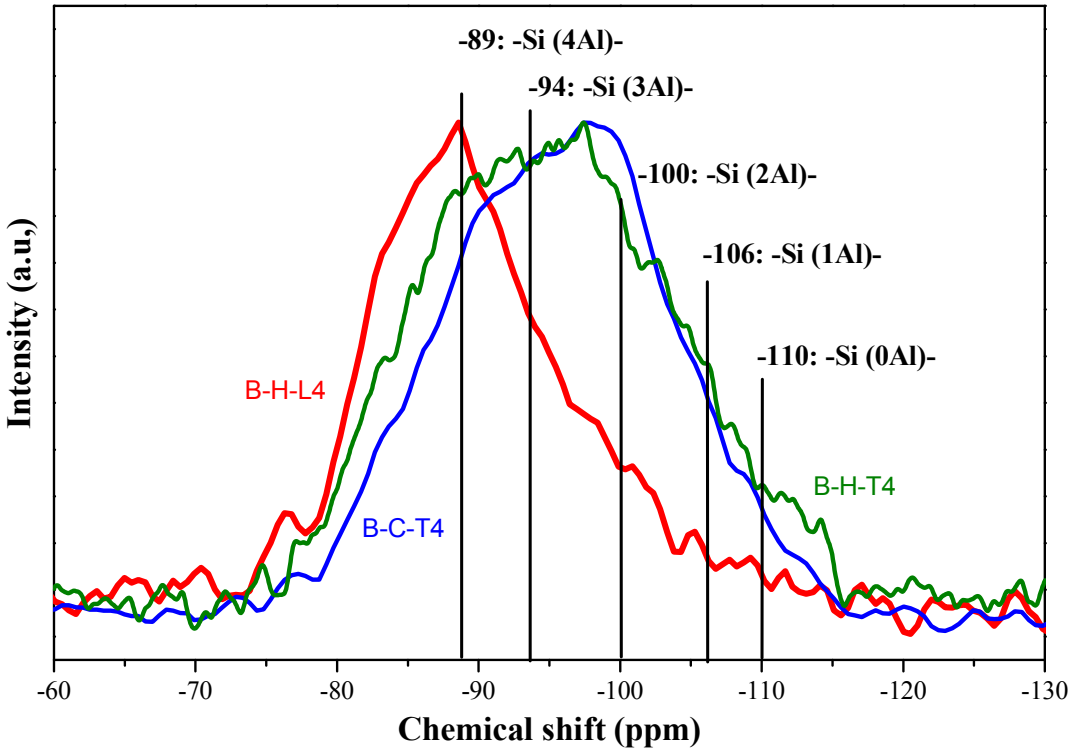

FIGURE 7

Published in Catalysis Today, 215 (2013) 208-215
DOI: 10.1016/j.cattod.2013.03.015 *http://www.elsevier.com/*

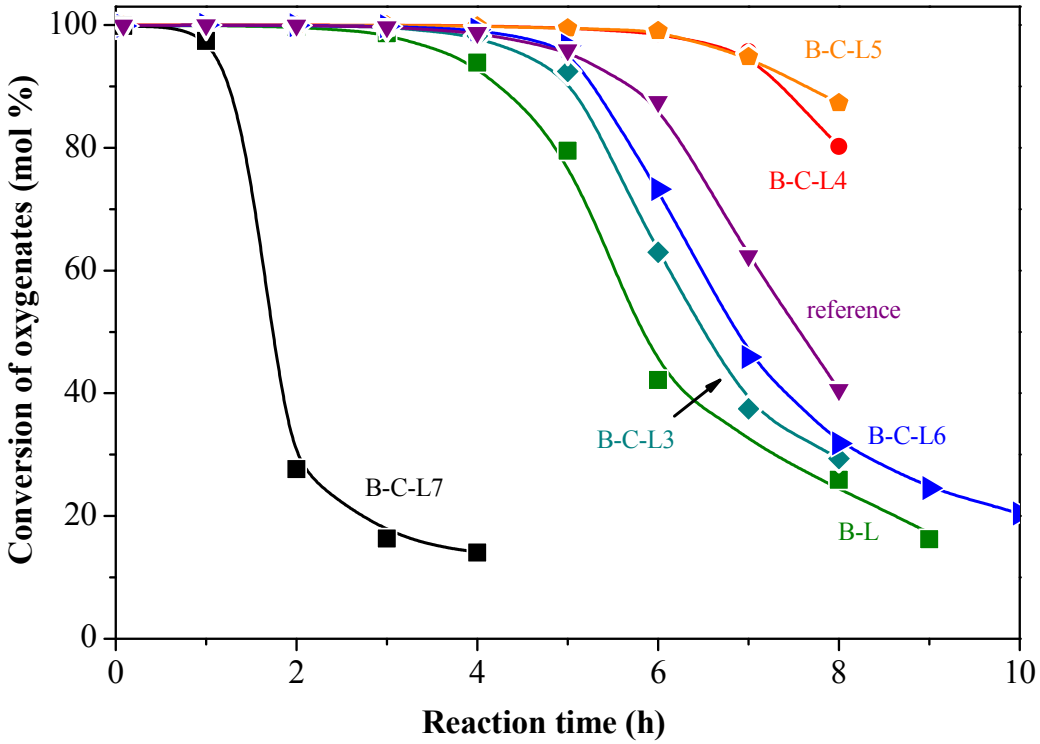

FIGURE 8

Published in Catalysis Today, 215 (2013) 208-215
DOI: 10.1016/j.cattod.2013.03.015 *http://www.elsevier.com/*

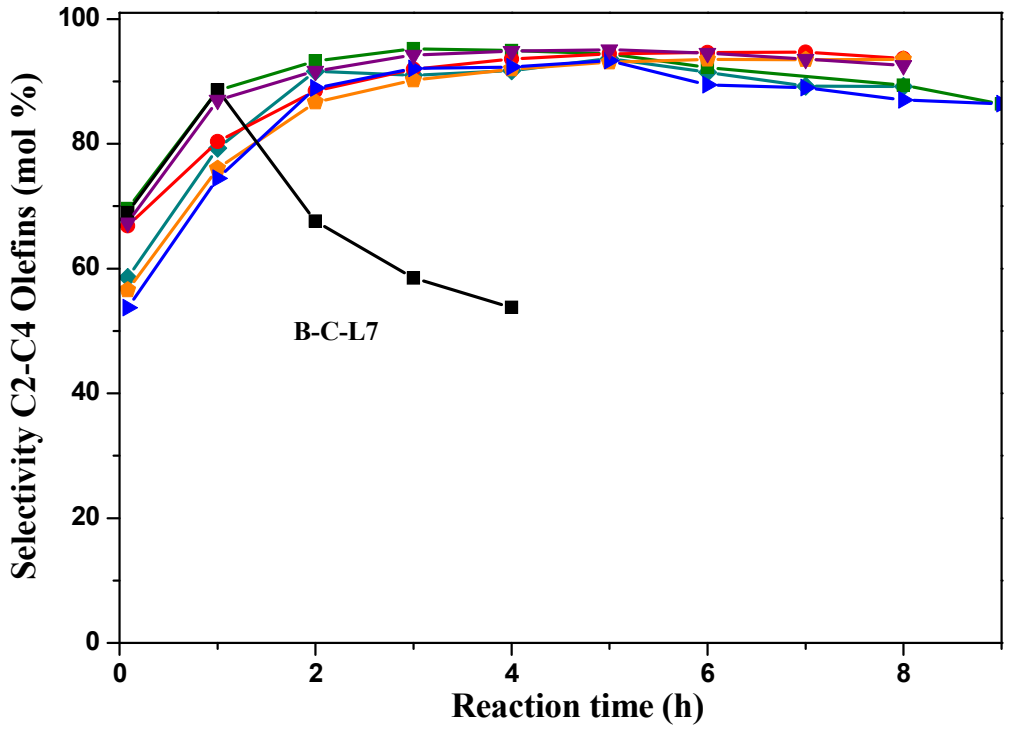

FIGURE 9

Published in Catalysis Today, 215 (2013) 208-215
DOI: 10.1016/j.cattod.2013.03.015 *http://www.elsevier.com/*

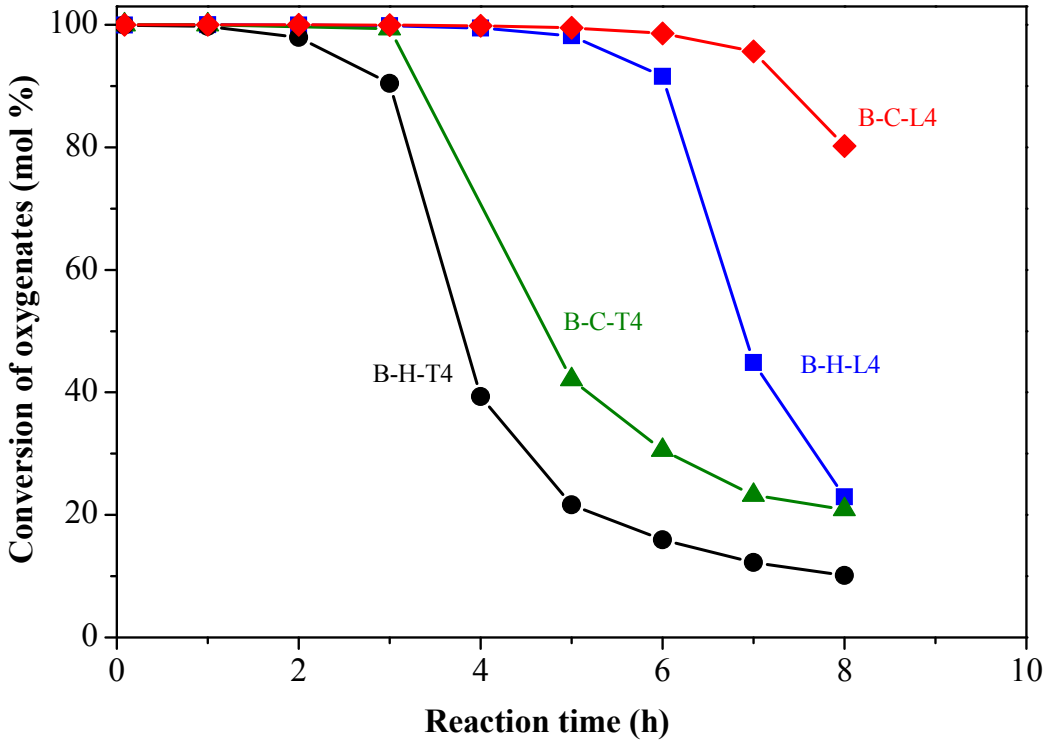

FIGURE 10

References

[1] J. Liang, H. Li, S. Zhao, W. Guo, R. Wang and M. Ying, Applied Catalysis, 64 (1990) 31.
[2] R. Vomscheld, M. Briend, M.J. Peltre, P.P. Man and D. Barthomeuf, Journal of Physical Chemistry, 98 (1994).
[3] E. Dumitriu, A. Azzouz, V. Hulea, D. Lutic and H. Kessler, Microporous Materials, 10 (1997) 1.
[4] Y.-J. Lee, S.-C. Baek and K.-W. Jun, Applied Catalysis A: General, 329 (2007) 130.
[5] G. Liu, P. Tian, J. Li, D. Zhang, F. Zhou and Z. Liu, Microporous and Mesoporous Materials, 111 (2008) 143.
[6] L. Ye, F. Cao, W. Ying, D. Fang and Q. Sun, Journal of Porous Materials, 18 (2010) 225.
[7] T. Álvaro-Muñoz, C. Márquez-Álvarez and E. Sastre, Catalysis Today, 179 (2012) 27.
[8] P. Wang, A. Lv, J. Hu, J.a. Xu and G. Lu, Microporous and Mesoporous Materials, 152 (2012) 178.
[9] D. Chen, K. Moljord, T. Fuglerud and A. Holmen, Microporous and Mesoporous Materials, 29 (1999) 191.
[10] S. Wilson and P. Barger, Microporous and Mesoporous Materials, 29 (1999) 117.
[11] Y. Hirota, K. Murata, S. Tanaka, N. Nishiyama, Y. Egashira and K. Ueyama, Materials Chemistry and Physics, 123 (2010) 507.
[12] I.M. Dahl, R. Wandelbo, A. Andersen, D. Akporiaye, H. Mostad and T. Fuglerud, Microporous and Mesoporous Materials, 29 (1999) 159.
[13] N. Nishiyama, M. Kawaguchi, Y. Hirota, D. Van Vu, Y. Egashira and K. Ueyama, Applied Catalysis A: General, 362 (2009) 193.
[14] H. van Heyden, S. Mintova and T. Bein, Chemistry of Materials, 20 (2008) 2956.
[15] J.-W. Jun, J.-S. Lee, H.-Y. Seok, J.-S. Chang, J.-S. Hwang and S.-H. Jhung, Bulletin of the Korean Chemical Society, 32 (2011) 1957.
[16] G. Sastre, D.W. Lewis and C.R.A. Catlow, Journal of Physical Chemistry, 100 (1996) 6722.
[17] G. Sastre, D.W. Lewis and C.R.A. Catlow, The Journal of Physical Chemistry B, 101 (1997) 5249.
[18] J. Tan, Z. Liu, X. Bao, X. Liu, X. Han, C. He and R. Zhai, Microporous and Mesoporous Materials 53 (2002).
[19] F.C. Sena, B.F. de Souza, N.C. de Almeida, J.S. Cardoso and L.D. Fernandes, Applied Catalysis A: General, 406 (2011) 59.
[20] Y. Iwase, K. Motokura, T.R. Koyama, A. Miyaji and T. Baba, Physical chemistry chemical physics : PCCP, 11 (2009) 9268.
[21] A. Izadbakhsh, F. Farhadi, F. Khorasheh, S. Sahebdelfar, M. Asadi and Y.Z. Feng, Applied Catalysis A: General, 364 (2009) 48.
[22] G. Sastre and D.W. Lewis, Journal of the Chemical Society, Faraday Transactions, 94 (1998) 3049.
[23] W. Shen, X. Li, Y. Wei, P. Tian, F. Deng, X. Han and X. Bao, Microporous and Mesoporous Materials, 158 (2012) 19.
[24] Y. Wei, D. Zhang, Z. Liu and B. Su, Journal of Catalysis, 238 (2006) 46.
[25] S. Bordiga, L. Regli, C. Lamberti, A. Zeccina, M. Bjorgen and K.P. Lillerud, Journal of Physical Chemistry B, 109 (2005) 7724.
[26] G.A.V. Martins, G. Berlier, S. Coluccia, P. H.O., G.B. Superti, G. Gatti and L. Marchese, Journal of Physical Chemistry C, 111 (2007) 330.
[27] L. Smith, A.K. Cheetham, L. Marechese, J.M. Thomas, P.A. Wright, J. Chen and E. Gianotti, Catalysis Letters, 41 (1996) 13.
[28] S. del Val, T. Blasco, E. Sastre and J. Pérez-Pariente, Journal of the Chemical Society, Chemical Communications, (1995) 731.
[29] M. Montoya-Urbina, D. Cardoso, J. Pérez-Pariente, E. Sastre, T. Blasco and V. Fornés, Journal of Catalysis, 173 (1998) 501.
[30] T. Blasco, A. Chica, A. Corma, W. Murphy, J. Agundez-Rodríguez and J. Pérez-Pariente, Journal of Catalysis, 242 (2006) 153.
[31] B.M. Lok, C.A. Messina, R.L. Patton, R.T. Gajek, T.R. Cannan and E.M. Flanigen, Crystalline silicoaluminophosphates US Patent 4 440 871, 1984.

[32] M. Zokaie, U. Olsbye, K.P. Lillerud and O. Swang, The Journal of Physical Chemistry C, 116 (2012) 7255.

Enhanced stability in the methanol-to-olefins process shown by SAPO-34 catalysts synthesized in biphasic medium

Teresa Álvaro-Muñoz, Carlos Márquez-Álvarez and Enrique Sastre*

Suplementary Information

Figure 1. XRD patterns before (red line) and after (blue line) calcination of different samples.

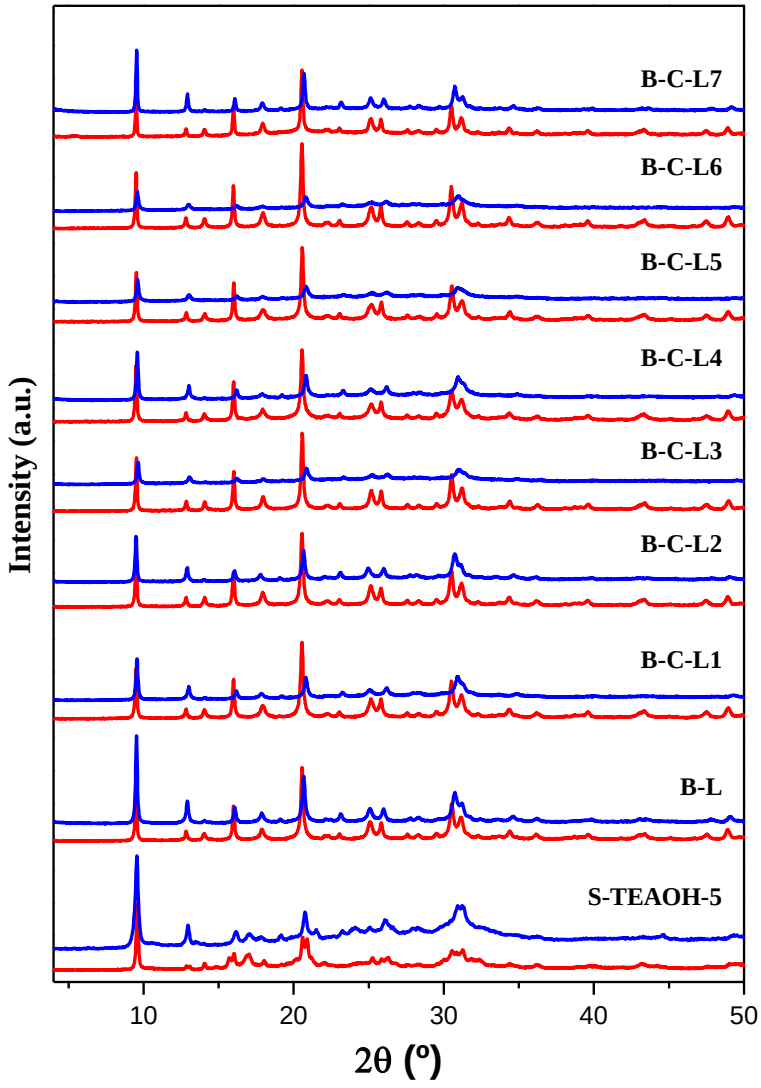

Figure 2. XRD patterns before (red line) and after (blue line) calcination of different samples.

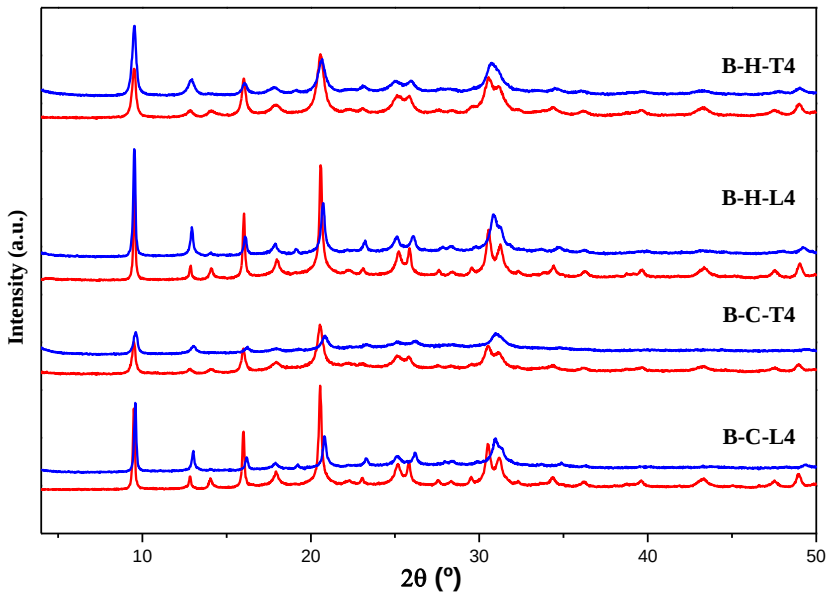

Figure 3. Nitrogen adsorption–desorption isotherms of different SAPO-34 samples acquired at 77 K.